Heart ablation using a planar rectangular high intensity ultrasound transducer and MRI guidance

Andreas Couppis [a,*], Christakis Damianou [b,c], Panayiotis Kyriacou [a], Cyril Lafon [d], Francoise Chavrier [d], Jean-Yves Chapelon [d], Alain Birer [d]

[a] City University, London, UK
[b] Frederick University Cyprus, Limassol, Cyprus
[c] MEDSONIC, LTD, Limassol, Cyprus
[d] INSERM, U556, Université de Lyon, Lyon F-69003, France

A B S T R A C T

The aim of this study was to evaluate a flat rectangular ($3 \times 10\,mm^2$) MRI compatible transducer operating at 5 MHz. The main task was to explore the feasibility of creating deep lesions in heart at a depth of at least 15 mm. The size of thermal necrosis in heart tissue was estimated as a function of power and time using a simulation model. The system was then tested in an excised lamb heart. In this study, we were able to create lesions of 15 mm deep with acoustic power of 6 W for an exposure of approximately 1 min. The contrast to noise ratio (CNR) between lesion and heart tissue was evaluated using fast spin echo (FSE). The CNR value was approximately 22 using T1 W FSE. Maximum CNR was achieved with repetition time (TR) between 300 and 800 ms. Using T2W FSE, the corresponding CNR was approximately 13 for the 14 *in vivo* experiments. The average lesion depth was 11.93 mm with a standard deviation of 0.62 mm. *In vivo* irradiation conditions were 6 W for 60 s. The size of the lesion in the other two dimensions was close to $3 \times 10\,mm^2$ (size of the transducer element).

Keywords:
Therapeutics
Hyperthermia
Ultrasound in surgery
Medical ultrasonics

Contents

1. Introduction

Arrhythmia is a problem with the speed or rhythm of the heartbeat. In this condition, the heart can beat too fast, too slow, or with an irregular rhythm. Most arrhythmias are harmless, but some can be serious or life threatening. With arrhythmia, the heart may not be able to pump enough blood to the body [1] Lack of blood flow can damage the brain, heart, and other organs. Atrial fibrillation (AF) and Ventricular Fibrillation (VF) are the most common types of serious arrhythmias.

AF is a very fast and irregular contraction of the atria. AF occurs when the heart's electrical signal begins in a different part of the atrium than the sinoatrial (SA) node or when the signal is conducted abnormally [1–3].

* Corresponding author. Address: 105 Evagora Laniti, 3111 Limassol, Cyprus. Tel.: +357 99460087.
E-mail address: acouppis@cytanet.com.cy (A. Couppis).

VF occurs when disorganized electrical signals make the ventricles quiver instead of pump normally. Without the ventricles pumping blood out to the body, a person will lose consciousness within seconds and will die within minutes if not treated [1] To prevent death, the condition must be treated immediately with defibrillation, an electric shock to the heart.

The Cox–Maze procedure is the gold standard for the surgical treatment of atrial fibrillation (AF) [4–7] Despite its efficacy, this procedure is not widely performed because of its complexity and technical difficulty. Recently, the introduction of ablation technologies has significantly changed this attitude. To simplify the operation, the incisions of the traditional cut and sew Maze procedure have been replaced with linear lines of ablation.

Ablation technologies have greatly simplified surgical approaches and have significantly increased the number of procedures being performed [8]. Various energy sources have been used clinically, including cryoablation, radiofrequency, microwave, laser, and high-frequency ultrasound. The goal of these devices is to create lesions to block activation wavefronts [8].

Cryoablation is unique among presently available technologies in that it destroys tissue by freezing instead of heating. The biggest advantage of this technology is its ability to preserve tissue architecture and collagen structure [9]. The potential disadvantage of this technology is the relatively long time necessary to create an ablation lesion (2–3 min). Also, the circulating blood volume acts as a heat sink which makes creating lesions in the beating heart difficult [9].

In electrophysiology laboratories, RF energy has been used for cardiac ablation for many years [10]. It is one of the first energy sources to be used in the operating room for AF ablation. The first team to use RF energy in humans was that of Borggrefe et al. [11] who disconnected a right-sided accessory pathway. Their pioneering work, which was subsequently been followed by many other teams, opened the door to transvenous ablation at a significantly lower risk compared with direct current (DC) ablation. This rendered RF ablation a widely applicable therapy for patients with supraventricular and ventricular arrhythmias. The efficacy of RF ablation is limited in cases which require the ablation of larger areas in thicker tissues, and when ablation is performed on the left side of the heart the risk of charring and thrombus formation becomes an issue, especially when high power settings and high target temperatures are used. A major advance in this area came after a long series of animal experiments mainly performed by Wittkampf [12] using irrigated tip RF ablation with closed or open irrigation.

Microwave ablation is an interesting technology that has several advantages over RF [13]. It is less likely to create char formation and is less sensitive to electrode positioning. It can reliably create transmural endocardial lesions, but it is not capable of creating epicardial lesions on the beating heart. Microwave ablation is an unfocused energy source that can cause collateral injury. This has been documented in case reports [13].

Laser ablation is a promising technology that may have some advantages over other energy sources [14–16]. The energy is focused, unaffected by overlying fat, and uses flexible fiber optics to deliver the energy to tissue. A disadvantage of this technology is that the energy delivery is unconfined and thus could cause collateral damage.

Therapeutic ultrasound, is a non-invasive extracorporeal technique capable of thermally ablating subsurface structures without injuring intervening tissues. Ultrasonic energy can be applied in a target volume to induce molecular agitation, absorptive heating, and ultimately thermal coagulative tissue necrosis. Therapeutic ultrasound offers several potential advantages over other therapy modalities. Unlike microwaves, it can be readily focused within small volumes. It does not have the cumulative risks associated with ionizing radiation, and it is unaffected by the optical opacities that block laser penetration. Furthermore, in contrast to radiofrequency (RF) waves, therapeutic ultrasound does not require direct contact with target tissue. The use of therapeutic ultrasound to create focal, ablative lesions in the heart has been reported in experimental models [17–19].

Therapeutic ultrasound was explored as a therapeutic modality in almost every accessible tissue. Several studies have examined the histological changes related to therapeutic ultrasound ablation in various tissues [20,19,21,22,18,23–27].

Within the last decade, therapeutic ultrasound has been used in various *in vitro* models [28–32]. Okumura et al. in 2008 [31], performed a study to examine tissue temperatures around pulmonary veins (PVs) during therapeutic ultrasound balloon ablation for atrial fibrillation. In 2009, Yokoyama and colleagues [30] developed a canine model of esophageal injury and left atrial-esophageal fistula after applications of forward-firing therapeutic ultrasound and side-firing unfocused ultrasound. Neven et al. in 2010 [29], evaluated an esophageal temperature (ET)-guided safety algorithm to apply therapeutic ultrasound in order to avoid severe complications with standard ablation of pulmonary vein isolation (PVI).

Therapeutic ultrasound has been used in various *in vivo* models for heart applications: Strickberger et al. in 1999 [18], carried out a study to determine whether therapeutic ultrasound can be used to ablate the atrioventricular (AV) junction within the beating heart. Their study suggested that therapeutic ultrasound produced well-demarcated lesions and appears to be a feasible energy source to create complete AV block within the beating heart without damaging the overlying or underlying cardiac tissue. Otsuka et al. [33] investigated the possibility of myocardial ablation in the left ventricle of beating dog hearts by monitoring treatment with 2-dimensional echocardiography. Recently a transesophageal ultrasound applicator was designed and evaluated with *in vivo* experiments [34,35] for the treatment of atrial fibrillation. The results indicated a potential application of the transesophageal ultrasound applicator for atrial fibrillation treatment.

Over the last decade, clinical studies have been conducted using commercially therapeutic ultrasound systems. Early study [36], revealed that, therapeutic ultrasound can create precise defects in different cardiac tissue without damage to the surrounding tissue. A multicenter clinical trial in 2005 [37], showed that after 6-month follow-up, epicardial, off-pump, beating-heart ablation with acoustic energy is safe and cures 80% of patients with permanent atrial fibrillation associated with long-standing structural heart disease.

A therapeutic ultrasound balloon catheter to isolate pulmonary veins (PVs) outside the ostia (PV antrum) was designed by Nakagawa et al. in 2007 [38]. Results of this study showed that forward-focused therapeutic ultrasound application isolated PVs outside the PV ostium with elimination of AF in 16 (59%) of the 27 patients at 12 months following the single ablation procedure. Another study by Schmidt et al. in 2009 [39] showed that, the novel defocused 12F Therapeutic Ultrasound-Ballon Catheter used in conjunction with a steerable sheath allows for very rapid pulmonary vein isolation (PVI) in patients with paroxysmal atrial fibrillation (PAF). Epicor cardiac ablation system [40,41] has been proven to be a concomitant procedure during open heart surgery that is safe and acceptably effective for the treatment of AF. Metzner et al. in 2010 [42], performed a clinical study for pulmonary vein isolation using first and second generation therapeutic ultrasound balloon catheters (ProRhythm, Ronkonkoma, NY, USA). Patients treated with symptomatic PAF showed long-term success rates similar radiofrequency current (RFC) ablation-based PVI procedures.

The combination of ultrasound and MRI was first cited by Jolez and Jakab [43] who demonstrated that an ultrasonic transducer can be used inside an MRI scanner. The concept of using MRI to monitor the necrosis produced by therapeutic ultrasound was demonstrated in the early 90's by Hynynen et al. [44] in canine

muscle. In the following years many studies have been conducted [45–50] showing that the contrast between necrotic tissue and normal tissue was excellent.

In this paper a flat rectangular MRI compatible transducer, $3 \times 10\ mm^2$, operating at a frequency of 5.3 MHz was used [51]. The aim was to create lesions in lamb heart *in vitro* and in rabbit *in vivo* using the cardiac transducer in order to measure the size of thermal necrosis in relation to the power and time. The experimental results are compared with the results of a simulation model.

Another task was to investigate the effectiveness of MRI in monitoring therapeutic protocols of therapeutic ultrasound in the heart. This was achieved with the optimization of MRI pulse sequences in order to maximize contrast between thermal necrosis and healthy cardiac tissue. Screening with MRI makes therapeutic ultrasound a more credible way of treatment in comparison to other ablation methods which are guided by X-rays. MRI offers a better contrast between thermal necrosis and healthy cardiac tissues, and offers the additional advantage that the patient will not be exposed to radiation. Therefore we have used the basic MRI sequences T1-W and T2-W fast spin echo (FSE). With T1-W FSE, the effect of repetition time (TR) on contrast was explored, whereas with T2-W FSE, the effect of echo time (TE) was explored.

The main innovation of this study is the evaluation of a planar MR compatible transducer in both *in vitro* and *in vivo* exploring the following 2 main issues:

(a) Acquire knowledge regarding the size of the lesion as a function of power and time (using simulation and experimental models) which could be used as a preliminary data for future clinical trials and
(b) Optimize the FSE MRI techniques for detecting the lesions created in heart tissue.

The advantage of using MRI is that the lesions can be monitored nearly in real time and therefore unwanted complications similar to what was reported by Metzner et al. in 2010 [42] can be avoided.

2. Materials and methods

2.1. HIFU/MRI system

Fig. 1 shows the block diagram of the therapeutic ultrasound/MRI system. The therapeutic ultrasound system consists of a signal generator (HP 33120A, Agilent technologies, Englewood, CO, USA), a RF amplifier (250 W, AR, Souderton, PA, USA), and a flat rectangular MR compatible transducer (Fig. 2).

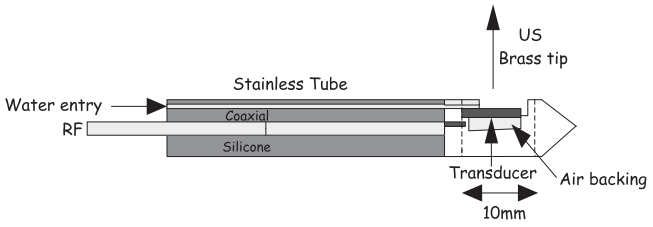

Fig. 2. Schematic of the flat rectangular MR compatible transducer.

The transducer consisted of a 3.8-mm outer diameter copper tube with a 0.1-mm thick wall ending in a cone-shaped MR compatible plastic tip. The plane active surface embedded in the plastic section is a $3 \times 10\ mm^2$ P762-type PZT piezoceramic air-backed transducer (Quartz & Silice, Nemours, France) operating at 5.3 MHz. In order to heat the myocardium for the purpose of treating arrhythmias, the transducer must be placed in a catheter. Because the catheter is guided to the myocardium through the arteries which are only 3–4 mm wide, the transducer element must be as compact as possible. If a spherically focused technology is used, then the size of the transducer will increase and therefore will not fit in the catheter. Also, because the catheter is inserted into the body, the catheter is destroyed after treatment (i.e. it is considered as consumable). Thus, a spherically focused technology has the additional disadvantage that will increase the cost substantially. Additionally, as it will be seen from the results, a flat transducer produces lesions of desired size.

The central lumen of the tube provided electrical radiofrequency (RF) connections and a path for the cooling water. RF connections were made via a miniaturized 50-cm long, 50 Ω coaxial cable with a 0.9-mm outer diameter. The outer ground conductor was connected to the external face of the transducer. The inner conductor reached the internal face of the transducer through the lumen of the tube. The transducer was glued with an MR compatible epoxy resin (Emerson & Cuming Europe nv, Westerlo-Oevel, Belgium) to ensure that it was watertight and to hold it in place. To limit energy loss during transmission of the electric signal, a connection with a capacitor-inductor network was included to match the transducer. Using the acoustic balance technique by

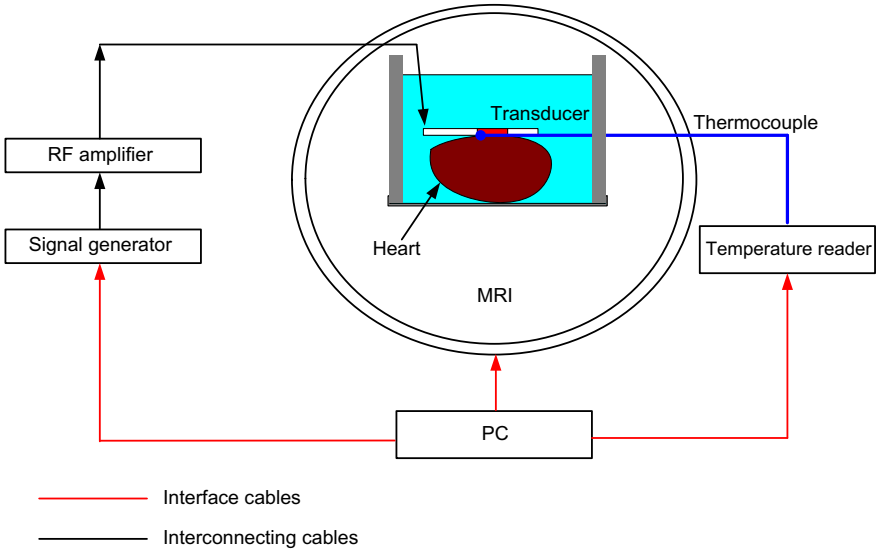

Fig. 1. Block diagram of the HIFU/MRI system used to drive the flat rectangular transducer.

Davidson 1991 [52], the electroacoustic efficiency of the applicator was measured to 65% at 5.3 MHz. The external face of the transducer was cooled by a continuous flow of degassed water circulating the length of the transducer. The cooling water serves as coupling medium between the transducer and the heated tissues. The water cooling circuit was maintained at 15 °C and was driven by a Masterflex peristaltic pump (Cole Parmer Instrument Co., Chicago, IL) at a flow of 0.15 L/min.

2.2. Simulation model

Numerical simulations were performed to predict the shape of the thermally ablated zone for different strategies, varying the following input parameters: thickness of the cooling water, the elementary sonication duration and the acoustical power. The model was proposed by Chavrier et al. 2000 [53] improved later by Curiel et al. 2004 [54]. It is based on the Bio Heat Transfer Equation proposed by Pennes [55]. Simulations neglected cavitation as the evaluated transducer is not focused and operates in the high frequency range.

The initial temperature of the heart was assumed to be 37 °C and the initial temperature of the water was assumed to be 15 °C. The spatial step used during the simulation was 0.5 mm and the temporal step used during the simulation was 0.1 s. The thermal dose threshold of necrosis was considered to be 240 min referenced at 43 °C.

The numerical model was implemented in C++ supported by a graphic user interface developed in MATLAB (MathWorks, Natick, United States). The simulation environment provided the following output: a 3D view plus two central sections of the predicted ablated zone, total volume of the coagulation necrosis and 3D map of estimated thermal dose.

Numerical simulations were performed for some exposures *in vivo* conditions (the tissue parameters used are shown in Table 1).

2.3. Temperature measurement

Temperature was measured using a Digital to analog data acquisition card (USB 6250, National Instruments, Austin Texas, USA) and a voltage to temperature converter (Omega Engineering, Stamford, Connecticut, USA). Temperature is sensed using a 50-μm diameter T-type copper-constantan thermocouple (Physitemp Instruments, Inc. New Jersey, USA) which is MRI compatible. The thermocouple was placed between the tissue and the transducer surface, thus measuring the temperature at the surface of the tissue. The temperature error of the thermocouple was on the order of 0.1 °C. In all the experiments, the goal was to keep the temperature below 100 °C in order to avoid boiling.

Table 1
Physical parameters used for simulations.

Parameter	*In vivo* values	
	Heart	Water
Thermal °conductivity (W m^{-1} °C^{-1})*	0.537*	0.627
Specific heat (J kg^{-1} °C^{-1})*	3720*	4188
Initial temperature (°C)*	37	10
Perfusion (kg m^{-3} s^{-1})*	14.2*	–
Density (kg m^{-3})*	1060	1000
Attenuation (Np m^{-1} MHz^{-1})*	4.1*	0

* Values taken from Duck FA. Physical properties of tissue. A comprehensive reference book. New York: Academic Press, 1990.

2.4. In vitro experiments

Various *in vitro* experiments were carried out to image the lesions using MRI created in cardiac tissue using therapeutic ultrasound. The tissue was placed inside the water container which was filled with degassed water at room temperature. The transducer was coupled to the holder and was immersed in the water tank, thus providing good acoustical coupling between tissue and transducer (see Fig. 1 for the experimental arrangement). In all experiments, the tissues used were extracted from freshly excised lamb, and the experiment was conducted in the same day. In total, 18 samples were used.

2.5. In vivo experiments

For the *in vivo* experiments, adult rabbits from Cyprus were used weighting approximately 3–4 kg. 14 rabbits in total were used in the experiments. The rabbits were anaesthetized using a mixture of 500 mg of Ketamine (100 mg/mL, Aveco, Ford Dodge, IA), 160 mg of Xylazine (20 mg/mL, Loyd Laboratories, Shenandoah, IA), and 20 mg of Acepromazine (10 mg/mL, Aveco, Ford Dodge, IA) at a dose of 1 mL/kg. The protocol for the animal experiments was approved by the national body in Cyprus responsible for animal studies (Ministry of Agriculture, Animal Services).

2.6. MRI processing

An MRI scanner (Signa 1.5 T, by General Electric, Fairfield, CT, USA) was used. The ultrasound transducer is coupled to the holder. The spinal coil (USA instruments, Cleveland, OH, USA) was used to acquire the MR.

The following parameters were used for T1-W FSE: TR was variable from 100 to 1000 ms, TE = 9 ms, slice thickness = 3 mm (gap 0.3 mm), matrix = 256 × 256, FOV = 16 cm, NEX = 1, and ETL = 8. For T2-W FSE: TR = 2500 ms, TE was variable from 10 ms to 160 ms, slice thickness = 3 mm (gap 0.3 mm), matrix = 256 × 256, FOV = 16 cm, NEX = 1, and ETL = 8.

The CNR was obtained by dividing the signal intensity difference between the Region of Interest (ROI) in the lesion and in the ROI of normal tissue by the standard deviation of the noise in the ROI of normal tissue. The ROI was circular with diameter of 3 mm.

3. Results

Fig. 3 shows T1 W FSE images of the 2 transducers utilized during the experiments in sagittal (Fig. 3A) and coronal (Fig. 3B) planes. Note the RF artefacts of the transducers are minimal. There is a 1 mm artefact around the transducer due to the copper material of the transducer and of the piezoelectric element.

Fig. 4A shows the lesion depth (experimental and simulated) as a function of time *in vitro* heart using acoustic power of 6 W. The spacing between the transducer and the heart tissue was 1 mm. The agreement between experimental and simulated results is excellent. Fig. 4B shows the lesion depth (experimental and simulated) as a function of power for a sonication duration of 35 s. The spacing between the transducer and heart tissue was also 1 mm. Based on the results of Fig. 4A it is concluded that in order to achieve 15 mm depth with acoustic power of 6 W exposure duration of 60 s is needed. From Fig. 4B it can be shown that to create a lesion of 15 mm 35 s are needed at a power of 9 W (Fig. 4B).

Fig. 5A shows a photograph of two lesions created in lamb heart *in vitro* at a plane perpendicular to the transducer beam axis. The power used was 6 W for 60 s. Note that the area of this lesion is slightly above the transducer area which is 10 × 3 mm^2. During

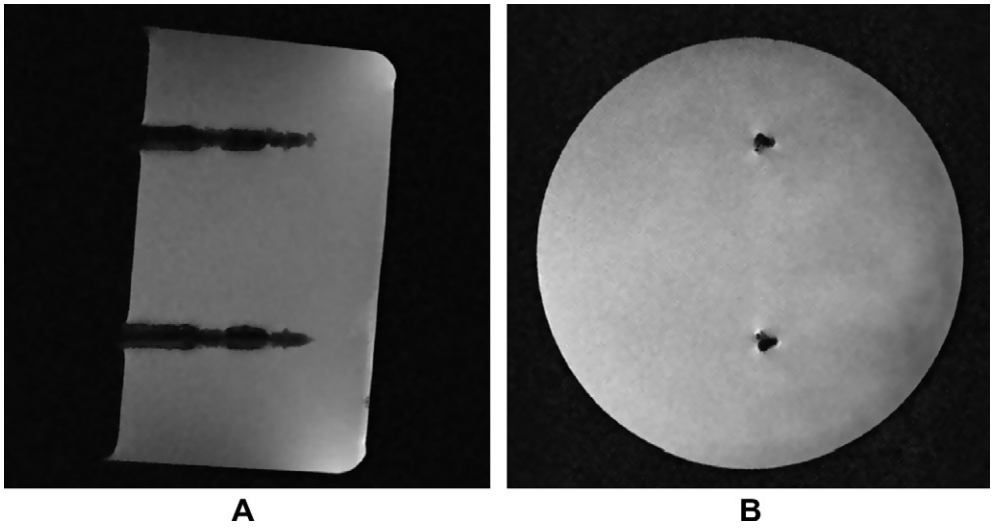

Fig. 3. T1 W FSE images of the 2 transducers utilized during the experiments in sagital (A) and coronal (B) planes.

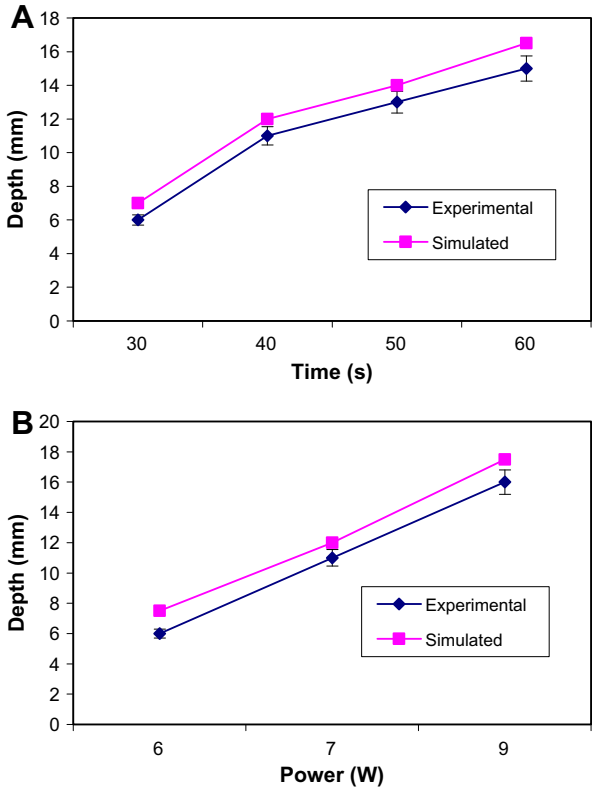

Fig. 4. (A) Depth of lesion (experimental and simulated) as a function of time *in vitro* heart using acoustic power of 6 W. The spacing between the transducer and heart tissue was 1 mm. (B), Depth of the lesion (experimental and simulated) as a function of power for sonication duration of 35 s. The spacing between the transducer and heart tissue was also 1 mm.

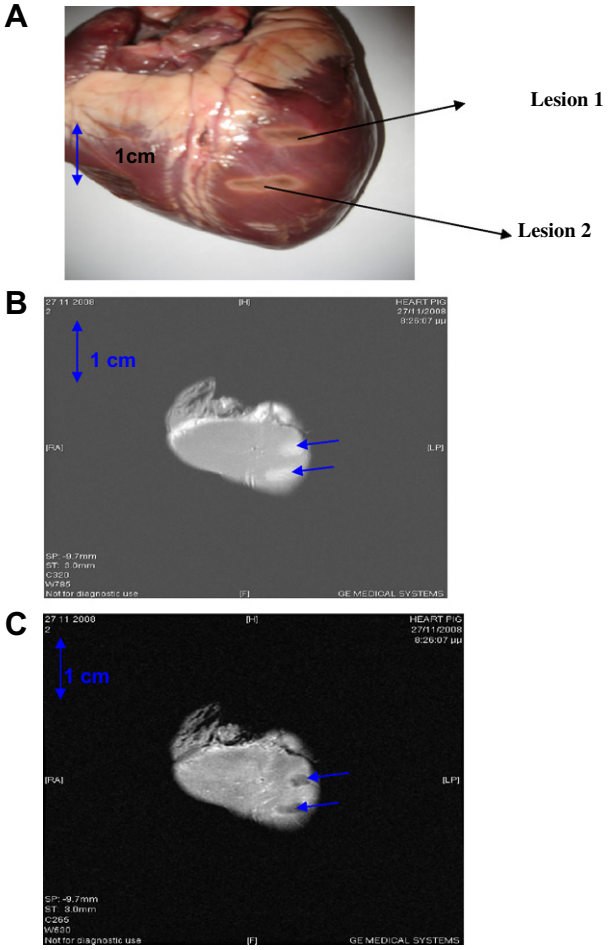

Fig. 5. (A) Photograph *in vitro* of two lesions created in lamb heart *in vitro* at a plane perpendicular to the transducer beam axis. The power used was 6 W for 60 s. (B). MRI image of the result of figure A using T1-W FSE for TR of 500 ms. (C). MRI image of the result of figure A using T2-W FSE with TE of 80 ms.

gross anatomy the lesion depth was close to 15 mm. Fig. 5B shows the MRI image of the result of Fig. 5A using T1-W FSE for TR of 500 ms. Note that the lesion appears much brighter than the heart tissue, resulting to good image contrast. Fig. 5C shows the MRI image of the result of Fig. 5A using T2-W FSE with TE of 80 ms. In the T2-W image the lesion appears darker compared to the heart tissue.

T1-W FSE was investigated further by using different TR (200–1000 ms with increment step of 100 ms) and T2-W FSE was investigated further by using different TE (20, 40, 60, 100, and 120 ms). Fig. 6A shows the contrast to noise ratio (CNR) of T1 FSE plotted against TR in lamb heart *in vitro*. Fig. 6B shows the contrast to noise

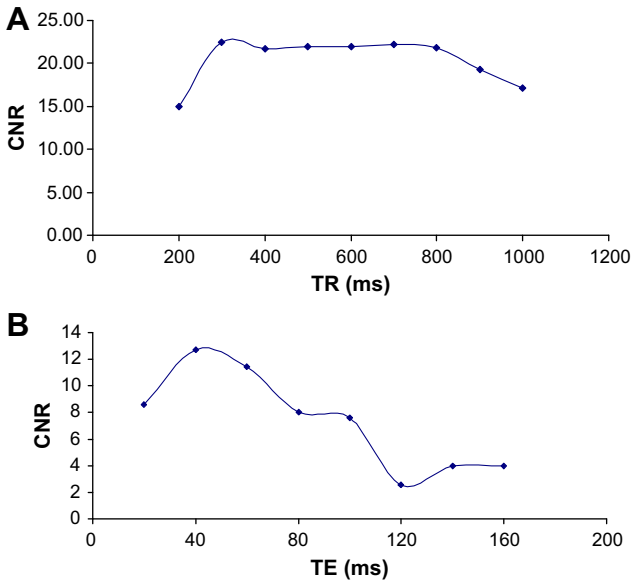

Fig. 6. (A) Contrast to noise ratio (CNR) of T1 FSE plotted against TR in lamb heart *in vitro*. (B). Contrast to noise ratio (CNR) of T2-W FSE plotted against TE in lamb heart *in vitro*.

ratio (CNR) of T2-W FSE plotted against TE in lamb heart *in vitro*. Note that the CNR with T2-W FSE is much lower than T1-W FSE.

Fig. 7A shows a photo of a lesion created in the heart of lamb tissue *in vitro* using 7 W at 35 s. The shape and size is in very good agreement with the lesion predicted by the simulation model (Fig. 7B). The experimental lesion depth was 10 mm, whereas the simulated lesion depth was 9.5 mm.

Fig. 8 shows a photo of a lesion created in the heart of rabbit *in vivo* using 7 W for 35 s. The area of the lesion in a plane parallel to the transducer follows the area of the transducer ($3 \times 10\ mm^2$). Despite of the motion of the heart and the high perfusion in the heart, it was feasible to obtained lesion size similar to what was obtain in the *in vitro* case ($3 \times 10\ mm^2$), however the penetration depth in the tissue was 12 mm compared to 15 mm (*in vitro* case). The thickness of this particular heart was 19 mm. The lesion was measured after the animal was sacrificed using a digital calliper.

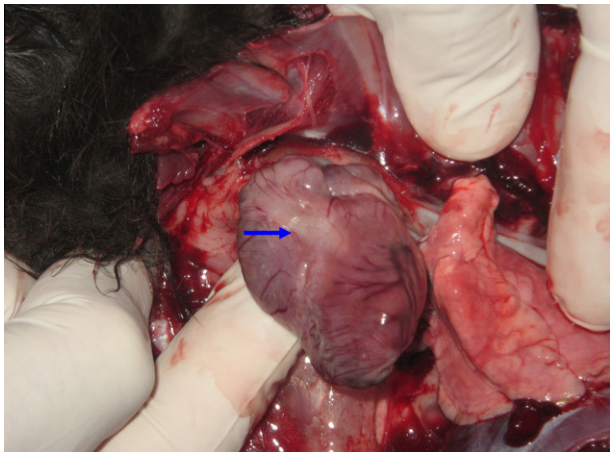

Fig. 8. Photo of a lesion created in the heart of rabbit *in vivo* using 6 W at 120 s.

Lastly, Fig. 9 shows the simulated depth vs. time at various levels of acoustic power. This figure essentially shows the main outcome of this study in one graph. It shows transducer (lesion depth) vs. the two main user-selected parameters (power and time). Note that the higher the power, the higher the rate of increase of lesion depth with time.

Fig. 10 shows the lesion depth created by the transducer using 6 W for 60 s for the various *in vivo* experiments. The mean lesion depth (excluding 2 experiments that failed due to possibly bad coupling) was 11.93 mm with a standard deviation of 0.62 mm.

4. Discussion

This paper presents a flat rectangular MR compatible transducer which can be used in the future to treat arrhythmias. This transducer was evaluated in lamb heart *in vitro* and in rabbit heart *in vivo*. A major part of the paper was to evaluate the performance of this transducer using a thermal simulation model. In this study, it is shown that the experimental and simulated results are in reasonable agreement, indicating that the theoretical model can be used to give guidelines for this type of transducer.

The target of this study was to create lesions of depth of at least 15 mm. This depth is sufficient to destroy unwanted electrical sig-

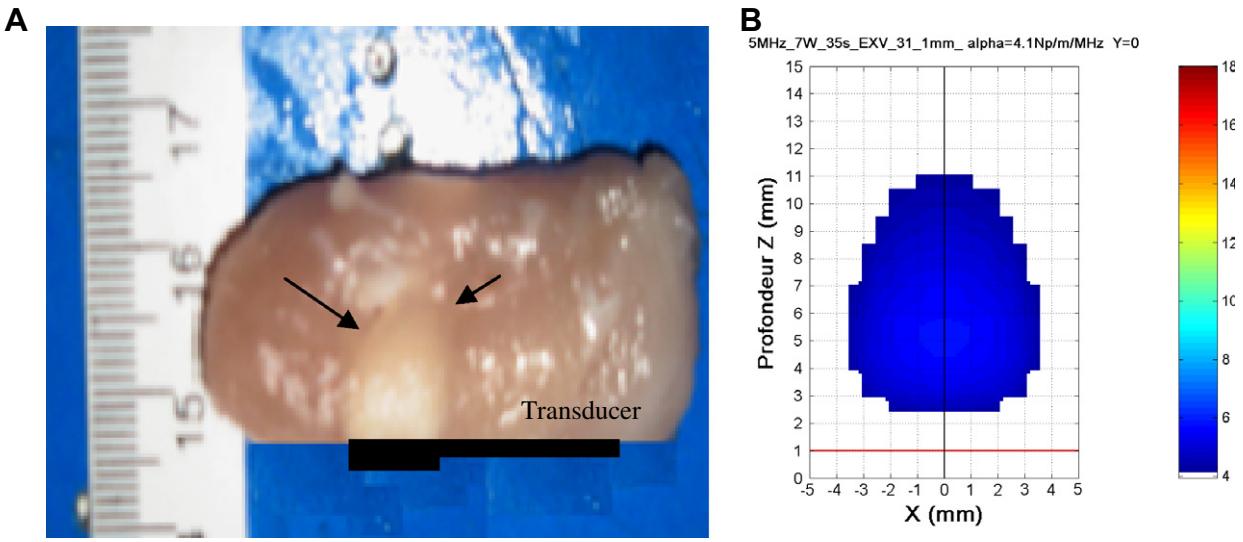

Fig. 7. (A). Photo of a lesion created in the heart of lamb tissue *in vitro* using 7 W for 35 s. (B). Simulated lesion for the exposure conditions of figure A.

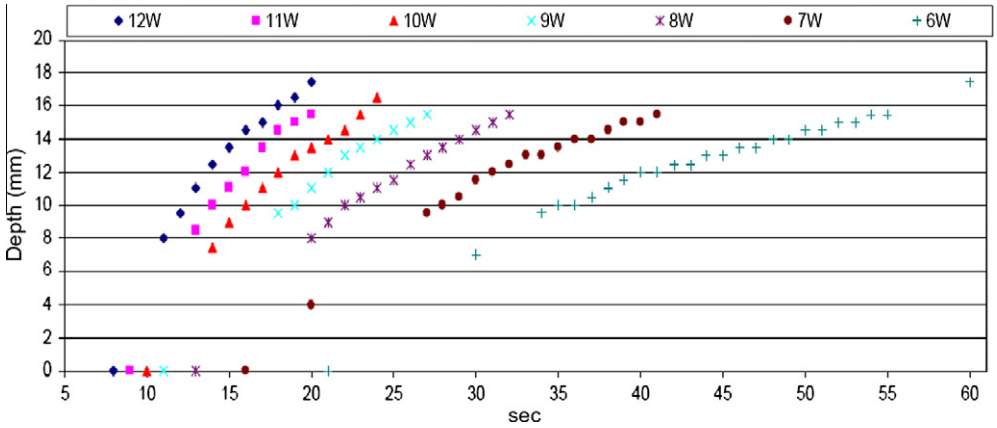

Fig. 9. Simulated depth vs. time at various levels of acoustic power.

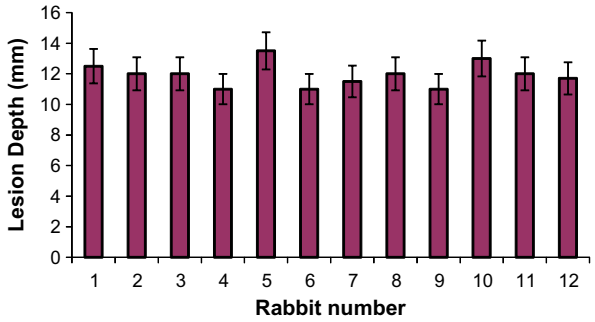

Fig. 10. Lesion depth created by the transducer using 6 W for 30 s for the various *in vivo* experiments. The mean lesion depth was 12.93 mm (standard deviation was 0.62 mm.

nals in the heart, and therefore treat arrhythmias. The size of necrosis in a plane parallel to the transducer face is always slightly higher than the transducer area (10×3 mm^2). The depth of lesions as expected increases with time, and the rate of increase of lesion depth with respect to time is higher for higher power. With increased acoustic power, the exposure duration needed to achieve the same lesion dimensions deep in the tissue is decreased. In future clinical trials, this transducer can be attached to a catheter, and with MRI it will be easy to guide and monitor treatment. MRI has the added advantage that offers a better contrast between thermal necrosis and cardiac tissue than ultrasound or X-rays.

The size of the lesion in a plane parallel to the transducer face as shown in Fig. 7A (experimental) or Fig. 7B (simulated) is 3×10 mm^2 (corresponds to the area of the transducer). At a deeper level, the size of the lesion becomes smaller. This is attributed to the fact that deeper in the tissue the intensity drops, and necessarily so does the temperature. As a result, the lateral conduction effect is lower and therefore the lesion size becomes smaller. If one needs a deeper lesion, then either the power or time has to be increased, taking care not to exceed temperatures above 100 °C. Increased ablation time means increased treatment time, however the ablation time (1 min per lesion) is low compared to the time needed to place in future clinical trials a catheter in the heart (30–60 min).

The transducer used produces lesions depth up to 15 mm. This shows that with this therapeutic ultrasound technology, the lesion size in cardiac tissue is larger than the lesions created with other ablation techniques, such as radio frequency [13]. We have chosen a transducer operating at the frequency of 5 MHz although a higher frequency transducer could be more beneficial [17]. Since this catheter is inserted in the body (i.e. it is consumable) going to higher frequency means a more expensive transducer. We use 5 MHz which is not very expensive and as we have proved the efficacy is not harmed.

There are many studies that predicted the size of the lesions as function of power and time (for example [54,56,57]). For example Damianou and Hynynen [56] evaluated the lesion size in dog muscle *in vitro*, Fagi et al. [57] performed a similar study in bovine in liver and Curiel et al. [54] have evaluated the lesion size in prostate. Therefore, for each application (in our case heart) and for every transducer (in our case planar) the lesion size has to be evaluated both using simulation and experimental models. This parametric information is very essential because when this technology is applied to humans the users should have an indicative knowledge of the lesion size.

The effect of perfusion is important especially using such long time duration (60 s). For example for 6 W and 60 s duration the *in vitro* experiments the depth of lesion is approximately 15 mm. Using the same exposure *in vivo*, the depth of lesion is 12 mm which is attributed to the perfusion effect [58].

In this paper the other major goal was to measure the CNR of FSE MRI sequences in detecting thermal lesions created by therapeutic ultrasound in heart. Both T1-W FSE and T2-W FSE have been proven successful for providing excellent contrast between rabbit heart and thermal lesion. The maximum contrast measured with T1-W FSE is approximately 22. With T1-W FSE the TR under which CNR is maximized is between 300 ms and 800 ms.

The trend of CNR vs. TR starts to increase then it becomes flat and then at high TRs it starts to decrease again. This trend is justified because at low TRs, the difference between signal intensity of lesion and tissue is low at short times and therefore CNR is lower. At higher TR the signal intensity of lesion and tissue reaches their maxima and therefore the signal difference is lower and hence the CNR drops again.

The maximum CNR measured with T2-W FSE is 13. With T2-W FSE the TE under which CNR is maximized is between 30 and 60 ms. The trend of CNR vs. TE starts to increase then it becomes flat and then at high TEs it starts to decrease again. The same explanation holds as in the case of T1-W FSE.

The cost of this prototype research unit (transducer, cabling and tubing for cooling) is approximately 1500 Euros. If the transducer, cabling and tubing for cooling are produced as a final product for clinical use in large quantities the cost could be close to 600 Euros. This figure puts the HIFU ablation catheter at a cost which is about 20% more expensive than the RF ablation catheter.

We still believe that with the use of MRI the treatment of arrhythmias has a clinical use (despite the complication mentioned

by Metzner et al. 2010 [42]), because with the near real time imaging, the result of the therapy can be monitored. Therefore it is too early to abandon this technology for treating arrhythmias. Maybe in the future we may come to the conclusion that MRI cannot monitor the heating effects in the beating heart precisely, however this must be determined in future MRI studies.

4.1. Future work

In vitro MRI experiments do not provide much value due to the fact that the MRI response of a living tissue is different from *ex vivo* tissue responses. Thus, more *in vivo* work has to be done, especially regarding the MRI evaluation of thermal lesions. Additional MRI routines have to be explored because the FSE sequences used are long and sensitive to motion and could not be the optimum routines in a beating heart.

The key advantage of MRI is its ability to map temperature. However, this is difficult in a beating heart. In this paper there was no attempt to map the temperature in the heart tissue using MRI, and therefore this a key future task.

References

[1] M.A. Brodsky et al., The history of heart failure predicts arrhythmia treatment efficacy: data from the antiarrythmics versus implantable defibrillators (AVID) study, Am. Heart J. 152 (2006) 724–730.

[2] S. Maltais, J. Forcillo, D. Bouchard, M. Carrier, R. Cartier, P. Demers, L.P. Perrault, N. Poirier, M. Ladouceur, P. Pagé, M. Pellerin, Long-term results following concomitant radiofrequency modified maze ablation for atrial fibrillation, J. Cardiac Surg. 25 (2010) 608–613.

[3] Pierre Jais, Michel Haissaguerre, Dipen C. Shah, Salah Chouairi, Laurent Gencel, Meleze Hocini, Jacques Clementy, A focal source of atrial fibrillation treated by discrete radiofrequency ablation, Am. Heart Assoc. 95 (1997) 572–576.

[4] S.M. Prasad, H.S. Maniar, C.J. Camillo, et al., The cox maze III procedure for atrial fibrillation: long-term efficacy inpatients undergoing lone versus concomitant procedures, J. Thorac. Cardiovasc. Surg. 126 (2003) 1822–1828.

[5] E. Raanani, A. Albage, T.E. David, et al., The efficacy of the cox/maze procedure combined with mitral valve surgery: a matched control study, Eur. J. Cardio.-Thorac. Surg. 19 (2001) 438–442.

[6] D.B. Doty, K.A. Dilip, R.C. Millar, Mitral valve replacement with homograft and maze III procedure, Ann. Thorac. Surg. 69 (2000) 739–742.

[7] H.V. Schaff, J.A. Dearani, R.C. Daly, et al., Cox–maze procedure for atrial fibrillation: mayo clinic experience, Semin. Thorac. Cardiovasc. Surg. 12 (2000) 30–37.

[8] H. Calkins, J. Brugada, D.L. Packer, R. Cappato, S.A. Chen, H.J. Crijns, et al., HRS/EHRA/ECAS expert consensus statement on catheter and surgical ablation of atrial fibrillation: recommendations for personnel, policy, procedures and follow-up. A report of the heart rhythm society (HRS) task force on catheter and surgical ablation of atrial fibrillation, Heart Rhythm 4 (2007) 816–861.

[9] F. Milla, N. Skubas, W.M. Briggs, et al., Epicardial beating heart cryoablation using a novel argon-based cryoclamp and linear probe, J. Thorac. Cardiovasc. 131 (2006) 403–411.

[10] N. Viola, M.R. Williams, M.C. Oz, N. Ad, The technology in use for the surgical ablation of atrial fibrillation, Semin. Thorac. Cardiovasc. Surg. 14 (2002) 198–205.

[11] M. Borggrefe, T. Budde, A. Podczeck, G. Breithardt, High frequency alternating current ablation of an accessory pathway in humans, J. Am. Coll. Cardiol. 10 (1987) 576–582.

[12] F.H. Wittkampf, Temperature response in radiofrequency ablation, Eur. Heart J. 86 (1992) 1648–1650.

[13] S. Geidel, M. Lass, J. Ostermeyer, A 5-year clinical experience with bipolar radiofrequency ablation for permanent atrial fibrillation concomitant to coronary artery bypass grafting and aortic valve surgery, Interact. Cardiovasc. Thorac. Surg. 7 (2008) 777–780.

[14] S.P. Thomas, D.J. Guy, A. Rees, et al., Production of narrow but deep lesions suitable for ablation of atrial fibrillation using a saline cooled narrow beam Nd:YAG laser catheter, Laser. Surg. Med. 28 (2001) 375–380.

[15] V.Y. Reddy, C. Houghtaling, J. Fallon, et al., Use of a diode laser balloon ablation catheter to generate circumferential pulmonary venous lesions in an open-thoracotomy caprine model, Pac. Clin. Electrophysiol. 27 (2004) 52–57.

[16] R.J. Darwood, N. Theivacumar, D. Dellagrammaticas, A.I. Mavor, M.J. Gough, Randomized clinical trial comparing endovenous laser ablation with surgery for the treatment of primary great saphenous varicose veins, Brit. J. Surg. 95 (2008) 294–301.

[17] D.S. He, J.E. Zimmer, F.I. Marcus, et al., Application of ultrasound energy for intracardiac ablation of arrhythmias, Eur. Heart J. 16 (1995) 961–966.

[18] S.A. Strickberger, T. Tokano, J.A. Kluiwstra, et al., Extracardiac ablation of the canine atrioventricular junction by use of high intensity focused ultrasound, Am. Heart Assoc. 100 (1999) 203–208.

[19] L.A. Lee, C. Simon, E.L. Bove, et al., High intensity focused ultrasound effect on cardiac tissues: potential for clinical application, Echocardiography 17 (2000) 563–566.

[20] C. Damianou, In vitro and in vivo ablation of porcine renal tissues using high-intensity focused ultrasound, Ultrasound Med. Biol. 29 (2003) 1321–1330.

[21] A.L. Malcolm, G.R. ter Haar, Ablation of tissue volumes using high intensity focused ultrasound, Ultrasound Med. Biol. 22 (1996) 659–669.

[22] A. Sibille, F. Prat, J.Y. Chapelon, et al., Characterization of extracorporeal ablation of normal and tumor-bearing liver tissue by high intensity focused ultrasound, Ultrasound Med. Biol. 19 (1993) 803–813.

[23] M. Susani, S. Madersbacher, C. Kratzik, L. Vingers, M. Marberger, Morphology of tissue destruction induced by focused ultrasound, Eur. Urol. 23 (1993) 34–38.

[24] N.I. Vykhodtseva, K. Hynynen, C. Damianou, Pulse duration and peak intensity during focused ultrasound surgery: theoretical and experimental effects in rabbit brain in vivo, Ultrasound Med. Biol. 20 (1994) 987–1000.

[25] F. Wu, W.Z. Chen, J. Bai, et al., Pathological changes in human malignant carcinoma treated with high-intensity focused ultrasound, Ultrasound Med. Biol. 27 (2001) 1099–1106.

[26] L. Chen, G. ter Haar, D. Robertson, J.P. Bensted, C.R. Hill, Histological study of normal and tumor-bearing liver treated with focused ultrasound, Ultrasound Med. Biol. 25 (1999) 847–856.

[27] R. Yang, N.T. Sanghvi, F.J. Rescorla, K.K. Kopecky, J.L. Grosfeld, Liver cancer ablation with extracorporeal high-intensity focused ultrasound, Eur. Urol. 23 (1993) 17–22.

[28] Ryo Otsuka, Kana Fujikura, Kumiko Hirata, Todd Pulerwitz, Yukiko Abe, Takeki. Suzuki, In vitro ablation of cardiac valves using high-intensity focused ultrasound, Ultrasound Med. Biol. 31 (2004) 109–114.

[29] K. Neven, B. Schmidt, A. Metzner, K. Otomo, D. Nuyens, T. De Potter, K.R. Chun, F. Ouyang, K.H. Kuck, Fatal end of a safety algorithm for pulmonary vein isolation with use of high-intensity focused ultrasound, Circ. Arrhythmia Electrophysiol. 3 (2010) 260–265.

[30] K. Yokoyama, H. Nakagawa, K.A. Seres, E. Jung, J. Merino, Y. Zou, A. Ikeda, J.V. Pitha, R. Lazzara, W.M. Jackman, Canine model of esophageal injury and atrial-esophageal fistula after applications of forward-firing therapeutic ultrasound and side-firing unfocused ultrasound in the left atrium and inside the pulmonary vein, Circ. Arrhythmia Electrophysiol. 2 (2009) 41–49.

[31] Y. Okumura, M.W. Kolasa, S.B. Johnson, T.J. Bunch, B.D. Henz, C.J. O'Brien, D.V. Miller, D.L. Packer, Mechanism of tissue heating during high intensity focused ultrasound pulmonary vein isolation: implications for atrial fibrillation ablation efficacy and phrenic nerve protection, J. Cardiovasc. Electrophysiol. 19 (2008) 945–951.

[32] D.J. Engel, R. Muratore, K. Hirata, R. Otsuka, K. Fujikura, K. Sugioka, C. Marboe, F.L. Lizzi, S. Homma, Myocardial lesion formation using high-intensity focused ultrasound, J. Am. Soc. Echocardiogr. 19 (2006) 932–937.

[33] Ryo Otsuka, Kana Fujikura, Yukio Abe, Kazue Okajima, Todd Pulerwitz, David J. Engel, Robert Muratore, Jeffrey A. Ketterling, Andrew Kalisz, Robert Sciacca, Charles Marboe, Genghua Yi, Jie Wang, Shunichi Homma, Extracardiac ablation of the left ventricular septum in beating canine hearts using therapeutic ultrasound, J. Am. Soc. Echocardiogr. 20 (2007) 1400–1406.

[34] J. Werner, E.J. Park, H. Lee, D. Francischelli, N.B. Smith, Feasibility of in vivo transesophageal cardiac ablation using a phased ultrasound array, Ultrasound Med. Biol. 36 (2010) 752–760.

[35] N.R. Villamizar, J.H. Crow, V. Piacentino, L.R. Dibernardo, M.A. Daneshmand, D.E. Bowles, M.A. Groh, C.A. Milano, Reproducibility of left atrial ablation with therapeutic ultrasound energy in a calf model, J. Thorac. Cardiovasc. Surg. 140 (2010) 1381–1387.

[36] L.A. Lee, C. Simon, E.L. Bove, R.S. Mosca, E.S. Ebbini, G.D. Abrams, A. Ludomirsky, High intensity focused ultrasound effect on cardiac tissues: potential for clinical application, Echocardiography 17 (2000) 563–566.

[37] J. Ninet, X. Roques, R. Seitelberger, C. Deville, J.L. Pomar, J. Robin, O. Jegaden, F. Wellens, E. Wolner, C. Vedrinne, R. Gottardi, J. Orrit, M.A. Billes, D.A. Hoffmann, J.L. Cox, G.L. Champsaur, Surgical ablation of atrial fibrillation with off-pump, epicardial, high-intensity focused ultrasound: results of a multicenter trial, J. Thorac. Cardiovasc. Surg. 130 (2005) 803–809.

[38] H. Nakagawa, M. Antz, T. Wong, B. Schmidt, S. Ernst, F. Ouyang, T. Vogtmann, R. Wu, K. Yokoyama, D. Lockwood, S.S. Po, K.J. Beckman, D.W. Davies, K.H. Kuck, W.M. Jackman, Initial experience using a forward directed, therapeutic ultrasound balloon catheter for pulmonary vein antrum isolation in patients with atrial fibrillation, J. Cardiovasc. Electrophysiol. 18 (2007) 136–144.

[39] B. Schmidt, K.R. Chun, A. Metzner, A. Fuernkranz, F. Ouyang, K.H. Kuck, Pulmonary vein isolation with high-intensity focused ultrasound: results from the therapeutic ultrasound 12F study, Europace 11 (2009) 1281–1288.

[40] S. Mitnovetski, A.A. Almeida, J. Goldstein, A.W. Pick, J.A. Smith, Epicardial therapeutic ultrasound cardiac ablation for surgical treatment of atrial fibrillation, Heart Lung. Circ. 18 (2009) 28–31.

[41] S. Schopka, C. Schmid, A. Keyser, A. Kortner, J. Tafelmeier, C. Diez, L. Rupprecht, M. Hilker, Ablation of atrial fibrillation with the epicor system: a prospective observational trial to evaluate safety and efficacy and predictors of success, J. Cardiothorac. Surg. 5 (2010) 5–34.

[42] A. Metzner, K.R. Chun, K. Neven, A. Fuernkranz, F. Ouyang, M. Antz, R. Tilz, T. Zerm, B. Koektuerk, E. Wissner, I. Koester, S. Ernst, S. Boczor, K.H. Kuck, B. Schmidt, Long-term clinical outcome following pulmonary vein isolation with therapeutic ultrasound balloon catheters in patients with paroxysmal atrial fibrillation, Europace 12 (2010) 188–193.

[43] F.A. Jolez, P.D. Jakab, Acoustic pressure wave generation within an MRI system: potential medical applications, J. Magn. Reson. Imag. 1 (1991) 609–613.
[44] K. Hynynen, C. Damianou, A. Darkazanli, E. Unger, J.F. Schenck, The feasibility of using MRI to monitor and guide noninvasive ultrasound surgery, Ultrasound Med. Biol. 19 (1993) 91–92.
[45] H.E. Cline, J.F. Schenck, K. Hynynen, R.D. Watkins, S.P. Souza, F.A. Jolesz, MRI-guided focused ultrasound surgery, J. Comput. Assist. Tomogr. 16 (1992) 956–965.
[46] E. Lecornet, H.U. Ahmed, C.M. Moore, M. Emberton, Conceptual basis for focal therapy in prostate cancer, J. Endourol. 24 (2010) 811–818.
[47] J. Rabinovici, Y. Inbar, A. Revel, Y. Zalel, J.M. Gomori, Y. Itzchak, E. Schiff, S. Yagel, Clinical improvement and shrinkage of uterine fibroids after thermal ablation by magnetic resonance-guided focused ultrasound surgery, Ultrasound Obstet. Gynecol. 30 (2007) 771–777.
[48] K.B. Pauly, C.J. Diederich, V. Rieke, D. Bouley, J. Chen, W.H. Nau, A.B. Ross, A.M. Kinsey, G. Sommer, Magnetic resonance-guided high-intensity ultrasound ablation of the prostate, Magn. Reson. Imaging 17 (2006) 195–207.
[49] I.P. Wharton, I.H. Rivens, G.R. Ter Haar, D.J. Gilderdale, D.J. Collins, J.W. Hand, P.D. Abel, N.M. de Souza, Design and development of a prototype endocavitary probe for therapeutic ultrasound delivery with integrated magnetic resonance imaging, J. Magn. Reson. Imaging 25 (2007) 548–556.
[50] X.D. Zhou, X.L. Ren, J. Zhang, G.B. He, M.J. Zheng, X. Tian, L. Li, T. Zhu, M. Zhang, L. Wang, W. Luo, Therapeutic response assessment of high intensity focused ultrasound therapy for uterine fibroid: utility of contrast-enhanced ultrasonography, Eur. J. Radiol. 62 (2007) 289–294.
[51] C.X. Deng, F. Qu, V.P. Nikolski, Y. Zhou, I.R. Efimov, Fluorescence imaging for real-time monitoring of therapeutic ultrasound cardiac ablation, Ann. Biomed. Eng. 33 (2005) 1352–1359.
[52] F. Davidson, Ultrasonic power balances, in: R.C. Preston (Ed.), Output Measurements for Medical Ultrasound, Springer, 1991, pp. 75–90.
[53] F. Chavrier, J.Y. Chapelon, A. Gelet, D. Cathignol, Modeling of high-intensity focused ultrasound-induced lesions in the presence of cavitation bubbles, J. Acoust. Soc. Am. 108 (2000) 432–440.
[54] L. Curiel, F. Chavrier, B. Gignoux, S. Pichardo, S. Chesnais, J.Y. Chapelon, Experimental evaluation of lesion prediction modelling in the presence of cavitation bubbles: intended for high-intensity focused ultrasound prostate treatment, Med. Biol. Eng. Comput. 42 (2004) 44–54.
[55] H.H. Pennes, Analysis of tissue and arterial blood temperatures in resting forearm, J. Appl. Physiol. 1 (1948) 93–122.
[56] C. Damianou, K. Hynynen, The effects of various physical parameters on the size and shape of necrosed tissue volume during ultrasound surgery, J. Acoust. Soc. Am. 95 (3) (1993) 1641–1649.
[57] F. Li, R. Feng, Q. Zhang, J. Bai, Z. Wang, Estimation of HIFU induced lesions in vitro: numerical simulation and experiment, Ultrasonics 44 (2006) 337–340.
[58] L. Chen, G. Ter Haar, C. Hill, M. Dworkin, P. Carnochan, H. Young, J. Bensted, Effect of blood perfusion on the ablation of liver parenchyma with high-intensity focused ultrasound, Phys. Med. Biol. 38 (11) (1993) 1661–1667.